Ceriotti, M., Heiligers, J., and McInnes, C.R. (2012) Novel pole-sitter mission concepts for continuous polar remote sensing. Proceedings of the SPIE - the International Society for Optical Engineering, 8533 . 85330P. ISSN 0277-786X

Copyright © 2012 SPIE

A copy can be downloaded for personal non-commercial research or study, without prior permission or charge

The content must not be changed in any way or reproduced in any format or medium without the formal permission of the copyright holder(s)

When referring to this work, full bibliographic details must be given

http://eprints.gla.ac.uk/75377/

Deposited on: 19th February 2013

Enlighten – Research publications by members of the University of Glasgow
http://eprints.gla.ac.uk

Novel pole-sitter mission concepts for continuous polar remote sensing

Matteo Ceriotti*, Jeannette Heiligers, Colin R. McInnes
Advanced Space Concepts Laboratory, University of Strathclyde
75 Montrose St., Glasgow G1 1XJ, United Kingdom

ABSTRACT

The pole-sitter concept is a solution to the poor temporal resolution of polar observations from highly inclined, low Earth orbits and the poor high latitude coverage from geostationary orbit. It considers a spacecraft that is continuously above either the North or South Pole and, as such, can provide real-time, continuous and hemispheric coverage of the polar regions. Despite the significant distance from the Earth, the utility of this platform for Earth observation and telecommunications is clear, and applications include polar weather forecasting and atmospheric science, glaciology and ice pack monitoring, ultraviolet imaging for aurora studies, continuous telecommunication links with polar regions, arctic ship routing and support for future high latitude oil and gas exploration. The paper presents a full mission design, including launch (Ariane 5 and Soyuz vehicles), for two propulsion options (a near-term solar electric propulsion (SEP) system and a more advanced combination of a solar sail with an SEP system). An optional transfer from the North Pole to South Pole and vice-versa allows viewing of both poles in summer. The paper furthermore focuses on payloads that could be used in such a mission concept. In particular, by using instruments designed for past deep space missions (DSCOVR), it is estimated that resolutions up to about 20 km/pixel in the visible wavelengths can be obtained. The mass of these instruments is well within the capabilities of the pole-sitter design, allowing an SEP-only mission lifetime of about 4 years, while the SEP/sail propulsion technology enables missions of up to 7 years.

Keywords: Polar observation; Pole-sitter; Space mission design; High-latitude coverage; Space systems design; Polar weather; Polar meteorology.

1. INTRODUCTION

Spacecraft in geostationary orbit (GEO) have demonstrated the significant benefits offered by continuous coverage of a particular region. However, GEO platforms can only provide their services in the equatorial and temperate zones, where elevation angles are sufficiently high. At higher latitudes, similar services are provided at present by mainly two types of conventional platforms: highly-eccentric, inclined orbits, or low or medium polar orbits.

The first class includes the well-known Molniya-type orbits: they exploit the oblateness of the Earth (effect of the J_2 term in the geopotential) to maintain the argument of the pericentre constant in time [1]. In order to achieve this condition, their inclination must be fixed at the critical value of 63.4°. This value is still relatively low to obtain a satisfactory coverage not only of the polar caps, but also of the high-latitude regions [2]. Due to their high eccentricity, the orbit apocentre is usually at a distance that is comparable to GEO, and therefore offers a hemispheric view of the Earth. However, an intrinsic limitation is the impossibility of providing continuous coverage over time: despite that the spacecraft spends a significant fraction of its orbital period around the orbit apocentre, the viewing conditions of the poles change continuously, and there is an interval of time in which the spacecraft is at the pericentre and coverage is not available. With an orbital period of approximately 12 hours, it has been shown that three to six Molniya spacecraft are necessary to provide satisfactory continuous coverage [3]. Recent research [4] has considered changing the critical inclination of the Molniya orbit to 90°, using a continuous acceleration generated by a solar electric propulsion (SEP) system for maintaining the orbit. However, a continuous and constant polar view is not available.

The second class of orbits largely consists of Sun-Synchronous orbits. Spacecraft in these orbits are used due to the high spatial resolution that they can provide. However, only a narrow swath is imaged at each polar passage, relying on multiple passages (and/or multiple spacecraft) for full coverage. For example, Landsat 7 (altitude of 705 km at 98.2°) completes just over 14 orbits per day, covering the entire Earth between 81 degrees north and south latitude every 16

* Currently at University of Glasgow, Systems Power and Energy Division, School of Engineering, James Watt Building South, Glasgow G12 8QQ, United Kingdom. Email: matteo.ceriotti@glasgow.ac.uk; phone: +44 141 330 6465

Sensors, Systems, and Next-Generation Satellites XVI, edited by Roland Meynart, Steven P. Neeck, Haruhisa Shimoda,
Proc. of SPIE Vol. 8533, 85330P · © 2012 SPIE · CCC code: 0277-786/12/$18 · doi: 10.1117/12.974604

Downloaded From: http://spiedigitallibrary.org/ on 02/14/2013 Terms of Use: http://spiedl.org/terms

days.* This results in a poor temporal resolution for the entire polar region, as different areas are imaged at different times, hence missing the opportunity to have a simultaneous and continuous real-time view of the pole. At present, these images are post-processed to make a composite image, which can be used, for example, for weather forecasting and wind vector prediction. However, the data that can be extracted is neither complete nor accurate [5].

To overcome these limitations, the ideal platform would be one constantly above one of the poles, stationary with respect to the Earth, in the same way as a GEO spacecraft is stationary above one point on the equator. In this position, the footprint of the spacecraft will be constantly at the pole, in the same way as the footprint of a geostationary spacecraft is constantly at some longitude on the equator. This spacecraft is known in literature as "pole-sitter", which uses low-thrust propulsion to maintain a position along the polar axis (see Figure 1). The pole-sitter is the only platform that can offer a truly continuous hemispheric view of one of the poles, enabling real-time imaging over the entire disc (Figure 1b). The first study of this concept was apparently made by Driver [6] in 1980.

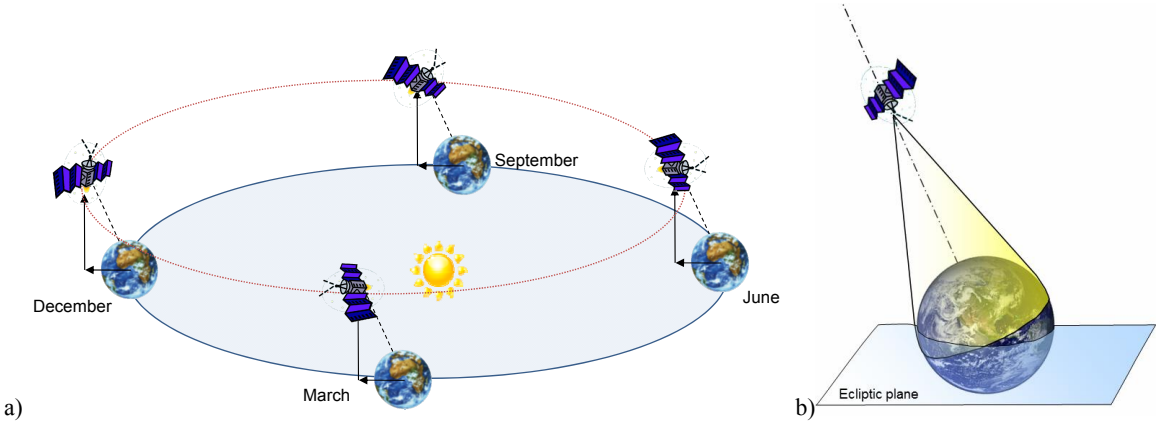

Figure 1. Pole-sitter concept in (a) Sun-centered inertial frame and (b) Earth-centered frame.

Driver proposed the use of solar electric propulsion (SEP) to maintain the pole-sitter position counterbalancing the gravitational forces. Despite the high efficiency of SEP, the thrusting time and hence the mission duration is always limited by the mass of propellant on-board.

In order to avoid this drawback, some authors investigated the use of a solar sail [7] instead of SEP as a means to provide the continuous acceleration. Solar sailing is a propellant-less spacecraft propulsion system that exploits the solar radiation pressure due to solar photons impinging on a large, highly reflecting surface (the sail) to generate thrust. Solar sails have been recently demonstrated in space [8, 9] and due to the interesting potential of providing acceleration without propellant mass, they seem to be suitable for potentially long duration missions that require a small, but continuous, thrust, such as the pole-sitter. One of the intrinsic limitations of solar sailing is the relationship between the direction of the sail force vector and its magnitude; in particular, the force can never be directed towards the Sun, which is the reason why a sailcraft cannot maintain the pole-sitter position indefinitely [10]. Other stationary positions in the Sun-Earth system [11] and non-Keplerian orbits [12] were studied in the literature, however the spacecraft does not achieve satisfactory conditions for continuous coverage of high-latitude regions.

In order to overcome the limitations of a platform based on a pure sail, which constrains the positions (or more generally the orbits) that can be achieved and maintained, hybrid propulsion has been proposed [13]. Hybridizing SEP and solar sailing is a comparatively recent idea [13], nevertheless research is flourishing in this field, investigating its potential for novel, interesting applications [14-18]. The reason for this interest is due to the fact that in the hybrid system, at the cost of increased spacecraft and mission design complexity, the two propulsion systems complement each other, cancelling their reciprocal disadvantages and limitations. While the hybrid propulsion pole-sitter can in principle enable a mission that is not feasible using only a solar sail and can extend the mission lifetime with respect to the pure SEP scenario, there are still issues associated with the pole-sitter mission related to the large distance from the Earth. As expected, the

* Landsat 7 Handbook, http://landsathandbook.gsfc.nasa.gov/ [Cited 17/08/2012]

Downloaded From: http://spiedigitallibrary.org/ on 02/14/2013 Terms of Use: http://spiedl.org/terms

acceleration required increases dramatically as the spacecraft is stationed closer to the Earth, and reasonable values of acceleration are obtained only if the Earth-spacecraft distance is of the order of millions of kilometers [6, 10]. Nevertheless, the advantage of having a static or quasi-static platform is such that these concepts are worth considering and investigating in more detailed studies [19]. Although high-bandwidth telecommunications and high-resolution imagery are difficult due to the large Earth-spacecraft distance, a number of novel potential applications are enabled, both in the fields of observation and telecommunications, which will be discussed in the paper. Due to these capabilities, and with the aim of increasing mission lifetime, the authors have undertaken an extensive investigation focused on the concept of a hybrid-propulsion pole-sitter: from the generation of optimal hybrid pole-sitter orbits [10], to system mass budgets [20], and from design of optimal transfers to the pole-sitter orbit from LEO [21], to design of optimal north-to-south transfers [22].

This paper presents the full mission and systems analysis of a pole-sitter mission, covering the launch phase and the operational phase. Several different options will be proposed and assessed, including different propulsion systems for the spacecraft (SEP or hybrid sail-SEP), different mission scenarios, enabling coverage of one pole only or both poles, and different launcher options. Then a systems design will determine the lifetime of the spacecraft, and some candidate payloads will be identified to enable the potential applications of the pole-sitter.

2. DYNAMICS AND SPACECRAFT ARCHITECTURES

2.1 Dynamics

The dynamics governing the motion of the spacecraft e consider a three-body problem in which the spacecraft is subject to the gravitational attraction of both the Earth and the Sun. This choice is made since the gravity of the Earth and the Sun are both important for a practical pole-sitter. In particular, we use the well-known circular restricted three-body problem (CR3BP) [23], which describes the motion of the spacecraft, of negligible mass, under the influence of the Sun and Earth (the *primaries*) that rotate in circular motion around each other (at a constant distance of 1.495978707×10^{8} km , or 1 Astronomical Unit). The reference frame is synodic, with its origin at the center-of-mass of the system, the x-axis passing through the Sun and the Earth, and oriented towards the latter, and the z-axis aligned with the angular velocity vector of the primaries, see Figure 2. The Earth rotates around the Sun with angular velocity $\boldsymbol{\omega} = 2\pi/\text{year}\ \hat{\mathbf{z}}$, which is also the angular velocity of the synodic frame.

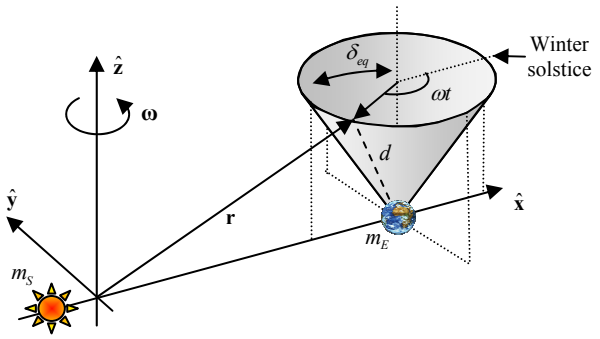

Figure 2. Synodic reference frame of the restricted three-body problem and pole-sitter reference.

A pole-sitter spacecraft is stationed along the polar axis of the Earth. We can consider that the direction of the polar axis of the Earth is inertially fixed while the Earth is orbiting the Sun (neglecting the nutation of the polar axis and the precession of the equinoxes). In the synodic ecliptic reference frame, the same axis rotates with a motion of apparent precession, due to the obliquity of the ecliptic: its angular velocity is $-\boldsymbol{\omega}$ (see Figure 2). Therefore, the polar axis spans a full conical surface every year, in a clockwise direction (refer again to Figure 2). The cone half angle is the tilt of the axis relative to the ecliptic, i.e. $\delta_{eq} = 23.5$ deg . The position of the spacecraft is to be constrained to follow the clockwise apparent precession of the polar axis, and hence maintain the pole-sitter condition. Figure 2 represents a particular north pole-sitter orbit in which the distance from the Earth $d(t)$ is constant. Without loss of generality, we consider the time $t_0 = 0$ as the winter solstice.

Downloaded From: http://spiedigitallibrary.org/ on 02/14/2013 Terms of Use: http://spiedl.org/terms

2.2 Spacecraft Architectures

We consider two different spacecraft architectures. The first is a pure SEP spacecraft, in which solar electric propulsion is used to provide the acceleration required throughout the mission. The spacecraft complexity is relatively low in this case, due to the high TRL of this type of propulsion system. The second is a more advanced, long-term spacecraft that exploits both solar sail and solar electric propulsion on the same bus.

2.2.1 Pure SEP

The pure SEP spacecraft can be considered as a conventional spacecraft with deployable solar arrays to power the propulsion system. Usually, the solar panels can be rotated along their longitudinal axis, so as to modulate the power delivered according to the instantaneous need of the spacecraft. The thruster is assumed to be rigidly connected to the spacecraft bus, and the thrust vector is steered by changing the attitude of the spacecraft (the instruments can be mounted on a gimbal).

The key technology parameters of an SEP thruster are the maximum thrust that it can provide, usually in the order of a fraction of a Newton, and its specific impulse. In this paper, we assume that the maximum thrust is used to size the SEP system, as will be explained later, and a fixed specific impulse of $I_{sp} = 3200$ s is conservatively assumed, based on current ion engine technology (existing NSTAR/DS1 [24] or EADS/Astrium RIT-XT [25]). It is foreseen that this specific impulse allows levels of thrust suitable for the spacecraft and mission under consideration. Higher values of specific impulse can be achieved with current SEP technology, for example, FEEP thrusters can provide specific impulses up to 10,000 s, but the thrust is limited to very small values of order 2 mN [26].

Since the fuel mass consumption is strictly related to the magnitude of the thrust, in general we will try to find trajectories that minimize propellant consumption, in order to maximize the mission lifetime, or alternatively, to maximize the payload mass for a given lifetime.

2.2.2 Hybrid Sail and SEP

In this scenario, we envisage the use of a spacecraft that combines solar sailing and SEP. As noted earlier, this adds system complexity, but it can be advantageous in terms of mission lifetime, as it will be shown in this paper.

The hybrid spacecraft has a bus from which the sail is deployed, and thus the sail is rigidly connected to it (see Figure 3). We assume that the sail can be steered, with relatively modest angular acceleration, by using the attitude control system of the spacecraft. The SEP thruster is also mounted on the spacecraft bus; however, for control purposes, it is required that the SEP thrust vector can steer independently of the sail orientation. Therefore the thruster shall be mounted on a gimbal system. Furthermore, the SEP system requires electrical power in order to operate. In conventional spacecraft, this is collected through solar arrays that are hinged on the spacecraft bus and can be oriented towards the Sun when power is needed. This type of architecture would be difficult to implement due to the presence of the sail. We instead envisage a layer of thin film solar cells (TFSC) which partly occupy the sail surface, similarly to the IKAROS spacecraft [27].

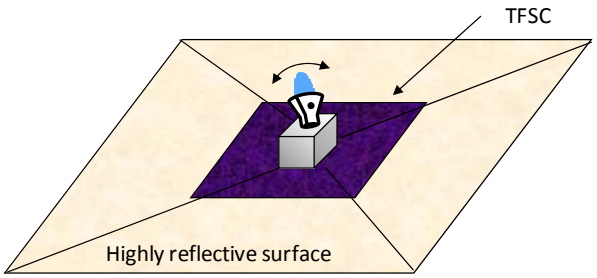

Figure 3. Hybrid spacecraft with sail, thin film solar cells and steerable thruster.

This paper assumes a partially absorbing solar sail (optical sail model) of total area A_s [7]. The sail acceleration varies with the inverse square distance from the Sun, and is directly proportional to the *system lightness number* β_0 (at pole-

Downloaded From: http://spiedigitallibrary.org/ on 02/14/2013 Terms of Use: http://spiedl.org/terms

sitter injection), which is a function of the sail loading $\sigma_0 = m_0/A_s$ of the spacecraft (spacecraft mass at pole-sitter injection over sail area):

$$\beta_0 = \sigma^*/\sigma_0$$

with $\sigma^* \cong 1.53 \cdot 10^{-3}$ kg/m^2 the critical sail loading. Values of β_0 up to 0.05 can be assumed for a near-term hybrid system [28]. Recent solar sail demonstrators, however, had considerably lower lightness numbers: JAXA's IKAROS [29] has a 20-m-diagonal square sail and weighs 350 kg ($\beta_0 = 0.001$), while NASA's NanoSail-D2 [9] is 4 kg for 10 m^2 ($\beta_0 = 0.003$). The lightness number (or alternatively σ_0) is an indicator of the technology needed for the spacecraft: the larger the lightness number is, the lower the sail loading is. This is achieved either using a larger sail area, or by reducing the system or sail mass.

The value of β_0 for the hybrid scenario can be decided following the study in Ref. [20]. That work showed that, if a sail assembly areal density, σ_s, of 10 g/m^2 is considered [28], then the hybrid spacecraft is beneficial only if very long missions are considered (i.e. lifetime > 7 years). Instead, considerable mass savings (or extended lifetime) are expected considering a mid- to far-term hybrid system with $\sigma_s = 5$ g/m^2 (or below) [30]. Furthermore, for this value, it is found that $\beta_0 = 0.035$ represents the lightness number in which the spacecraft initial mass, for a given payload, is lowest over a range of mission lifetimes. For these reasons, we select for this scenario: $\beta_0 = 0.035$, $\sigma_s = 5$ g/m^2.

The sail acceleration depends also on the reflectivity of the sail (0.9) and the thin film (0.4) [13, 14], and we consider that the latter cover an area $A_{TF} = 0.05A$ on the sail. This area ratio is a conservative estimation based on previous studies [14] and the IKAROS mission [29]. The actual value of this area depends on the spacecraft technology parameters, as well as the selected orbit, and will be computed in Section 3.2.

The controls of the hybrid spacecraft are the SEP thrust vector (three components), and additionally the sail attitude (two angular components). Therefore, optimal trajectories are those in which the sail is tilted such that the SEP acceleration is minimized.

3. MISSION DESIGN

The complete pole-sitter mission is split into different phases, schematically represented in Figure 4. The mission starts with a launch and transfer phase. This phase begins with the spacecraft injected into a low Earth orbit (LEO) by the launcher. An optimization process then optimizes a number of impulsive maneuvers that are performed using the launcher upper-stage. The upper-stage is then jettisoned and the spacecraft continues the transfer using its own low-thrust propulsion system, up to the injection point into the pole-sitter orbit.

At this point, the operational phase begins. The operational phase is the one in which the spacecraft is stationed along the polar axis of the Earth, and therefore the spacecraft is fully operational. This is obviously the most important phase of the mission, and the duration for which the spacecraft maintains this position shall be maximized to maximize the mission scientific return.

Since each pole is lit only 6 months per year, it is an option, especially for observations in the visible part of the spectrum, to transfer the spacecraft from a North Pole operational orbit to a symmetric orbit below the South Pole, and vice-versa, according to their lighting conditions. Therefore, an additional north-to-south transfer phase is designed. This phase can be inserted at appropriate points along the nominal orbit to enable the transfer to the other pole, where a symmetric operational orbit can be followed.

These three phases will be described and designed sequentially, starting from the operational phase, which defines the optimal nominal orbit. Then, the transfer from Earth to this orbit will be designed. The optimization of the transfer allows the determination of the maximum mass at the pole-sitter orbit injection, and therefore the spacecraft can be sized and the lifetime assessed. Finally, the north-to-south transfers will be designed, between optimal pole-sitter orbits.

The design of the three phases requires the solution of optimal control problems, which are solved numerically using a direct method based on pseudospectral transcription, implemented in the tool PSOPT, coded by Becerra [31].

Downloaded From: http://spiedigitallibrary.org/ on 02/14/2013 Terms of Use: http://spiedl.org/terms

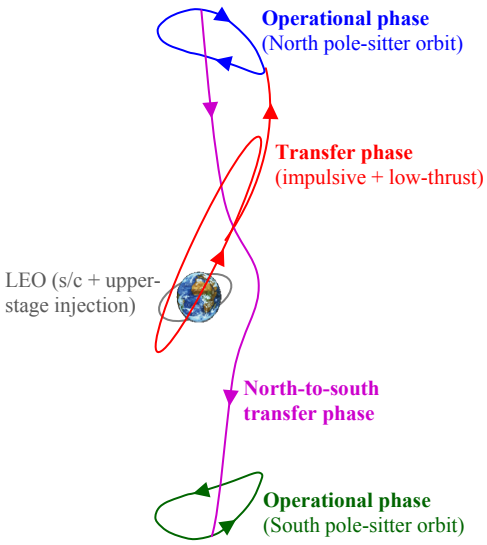

Figure 4. Representation of the mission phases.

3.1 Pole-Sitter Operational Orbits

An optimal pole-sitter orbit is defined as the one that minimizes the propellant consumption of the spacecraft, while maintaining the pole-sitter condition at any time, and being one-year periodic. The design of this orbit requires the (numerical) solution of a constrained optimal control problem, in which the control and state history over time is to be determined. Details of the optimization process are presented in Ref. [10].

In the optimization process, the distance from the Earth can vary, however a maximum is set to $d_{max} = 0.01831$ AU, i.e. 2.74 million km, in order to prevent the trajectory from going too far away from the Earth, thereby excessively decreasing the spatial resolution for instruments or the data bandwidth of the platform. In fact, it was found [10] that optimal, unconstrained trajectories move further away from the Earth in summer, which is the period in which the North Pole is lit, and therefore observations at optical wavelengths can be performed.

The result of the optimization, for the two scenarios, is presented in the following figures. Note that the figures showing the orbits (or later on in the paper, the transfers) employ a Sun-Earth synodic reference frame centered at the Earth rather than at the Sun-Earth barycenter for interpretation purposes. The optimal SEP-only path is essentially symmetric around spring and autumn, and the spacecraft is closest to the Earth at the summer and winter solstices. Instead, in the hybrid case, the spacecraft is closest to the Earth in winter and farthest in summer: the constraint on the maximum distance is active across the summer solstice for approximately 150 days. This can be seen in Figure 5. The same figure also highlights that the SEP spacecraft distance to Earth varies between 0.01568 and 0.01831 AU, while for the hybrid case it varies between 0.01369 and 0.01831 AU.

It results also that the SEP acceleration required is less for the hybrid spacecraft than for the pure SEP spacecraft. This is expected, as the sail provides a beneficial contribution to the total acceleration, and results in propellant mass saving. For example, for a spacecraft of mass 1000 kg at injection, the maximum SEP thrust would be 170 mN for the pure SEP system, and 144 mN for the hybrid system. At this point, however, the spacecraft mass is still unknown: it will be determined by the launcher capability and the transfer phase.

Downloaded From: http://spiedigitallibrary.org/ on 02/14/2013 Terms of Use: http://spiedl.org/terms

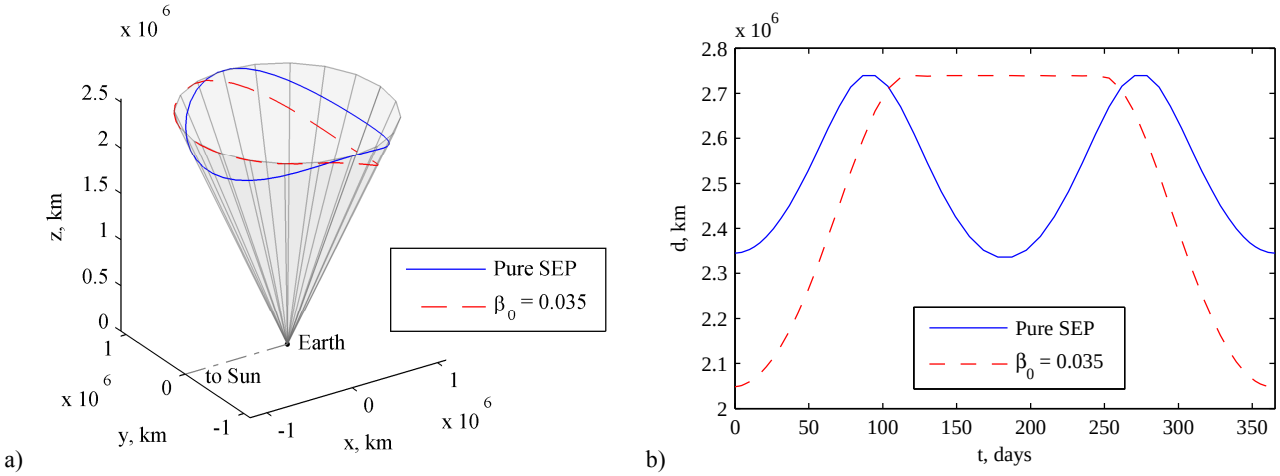

Figure 5. Fuel-optimal pole-sitter orbits for the pure SEP case and the hybrid case. (a) Optimal trajectories in the synodic reference frame. (b) Distance from the Earth.

3.2 Launch and Transfer Phase

In order to find the maximum mass that can be inserted into the pole-sitter orbit, this section investigates optimum transfers from LEO up to insertion into the pole-sitter orbit. The transfer is modeled as a launch phase and a transfer phase, as shown in Figure 4. The launch phase is designed as an impulsive, two-body Soyuz or Ariane 5 upper-stage transfer from a low Earth parking orbit up to insertion into the transfer phase. The transfer phase is modeled in the Earth-Sun three body problem using either pure SEP or hybrid propulsion, depending on the system architecture. The overall objective is to maximize the mass upon insertion into the pole-sitter orbit, assuming that the full launch vehicle capacity into the parking orbit is used. More details on this approach can be found in Ref. [21] . Table 1 provides data of the Soyuz and Ariane 5 parking orbits, as well as performances in terms of mass deliverable to these parking orbits and characteristics of their upper stages.

Table 1. Soyuz and Ariane 5 parking orbit and launch vehicle specifications

Launcher	Parking orbit			Upper stage		Adapter
	Altitude, km	Inclination, deg	Performance, kg	Mass, kg	Specific impulse, s	Mass, kg
Soyuz	200	51.8	7185	1000	330	100
Ariane 5	400	51.6	19000	4540	446	160

The resulting optimal transfers inject the spacecraft into the operational orbit at winter solstice, i.e. at the point closest to the Earth. More details on the optimal transfers, including the maximum thrust magnitude and mass injected into the pole-sitter orbit can be found in Table 2.

Since the SEP and hybrid pole-sitter orbits are not the same, a direct comparison of the performances of the transfers using the two propulsion techniques cannot be made. However, the mass injected into the hybrid pole-sitter orbit is larger than for the SEP case: an increase of 58 kg for a Soyuz launch and an additional 160 kg for an Ariane 5 launch. Part of this better performance will be due to the smaller Earth to pole-sitter distance at winter solstice (i.e. upon injection) for the hybrid pole-sitter orbit. However, part will also be due to the smaller propellant consumption in the transfer, because the hybrid case allows for a much longer duration in which the SEP thruster is switched off due to the contribution of the solar sail. However, the total transfer duration is considerably longer.

Downloaded From: http://spiedigitallibrary.org/ on 02/14/2013 Terms of Use: http://spiedl.org/terms

Table 2. Results for the optimization of transfer to SEP and hybrid low-thrust pole-sitter orbits including the maximum SEP thrust magnitude and the mass injected into the pole-sitter orbits.

Architecture	Launcher	Transfer time, d	T_{max} , N	m_0 , kg
SEP	Soyuz	79	0.269	1537
SEP	Ariane 5	79	0.775	4439
Hybrid	Soyuz	161	0.231	1595
Hybrid	Ariane 5	161	0.667	4599

3.3 Transfers between North and South Poles

Due to the tilt of the Earth's polar axis with respect to the ecliptic plane, the North and South Poles are alternately situated in darkness for 6 months per year. For observations being performed in the visible part of the spectrum (e.g. using the SSI, HRI or EPIC instruments of Table 5), this significantly constrains the mission scientific return. Therefore, an additional transfer is introduced that allows the pole-sitter spacecraft to change between pole-sitter orbits above the North and South Poles before the start of the Arctic and Antarctic winters, see Figure 4. For that, the SEP and hybrid pole-sitter orbits shown in Figure 5 are mirrored in the ecliptic plane. Viewed in the synodic frame, the Poles are illuminated when the spacecraft is in the Sun-ward part of the pole-sitter orbit, see Figure 6. Ideally, this means that the pole-sitter spacecraft would follow the north pole-sitter orbit from March to September and the south pole-sitter orbit from September to March. Clearly in reality this is not feasible since some time needs to be allowed for the spacecraft to transfer from north to south and vice-versa. Instead, departure takes place between summer and autumn (June – September), while arrival takes place between autumn and winter (September – December), see Figure 6, where this paper conventionally refers to the seasons in the northern hemisphere.

The concept of transfers between north and south pole-sitter orbits has been introduced before [22], and is applied in this section to the optimal SEP and hybrid pole-sitter orbits of Figure 5 (using the respective types of propulsion to perform the transfer). Also, for both propulsion strategies, both the Soyuz and Ariane 5 launch cases will be considered together with the corresponding values for the maximum thrust magnitude as provided in Table 2.

Note that due to the symmetry of the problem, the optimal transfers from north to south can also be used to transfer from south to north.

In the transfer design, a tradeoff has to be made between the observation time on the operational orbit (which shall be maximized), and the propellant consumption required for the transfer: a fast transfer guarantees long observation times, but requires more propellant.

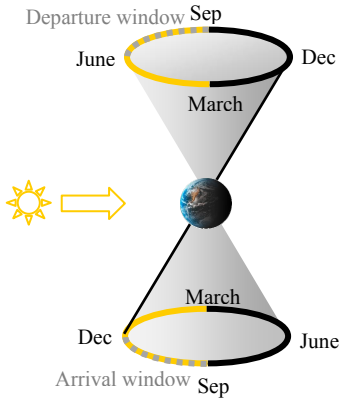

Figure 6. Schematic of dark (black line) and light (yellow line) conditions on the North and South Poles during the year and departure and arrival window (dotted) for a north-to-south transfer.

Downloaded From: http://spiedigitallibrary.org/ on 02/14/2013 Terms of Use: http://spiedl.org/terms

For the pure SEP spacecraft, a transfer that guarantees about 90 days of observation time in the operational orbit per year for each Pole uses as much propellant as the operational orbit itself. If the minimum-propellant (i.e. longest) transfer is used, the observation time reduces to 54 days, however the gain in propellant mass is 279.6 kg after 5 years, with respect to staying on the same pole-sitter orbit. On the other end, observation times of up to 94 days can be achieved, by using the quickest transfer. This comes, however, at the cost of an increase in the propellant consumption (45.3 kg more are required over 5 years). Very similar results are obtained for the hybrid case. Note that in the following, the minimum-propellant transfers are used.

3.4 Full Mission Profile

To illustrate the full mission profile, Figure 7 and Figure 8 represent the trajectory of the pole-sitter spacecraft, including the launch phase, operational phases and north-to-south transfers: Figure 7 refers to the pure SEP mission and Figure 8 to the hybrid propulsion one. Both figures represent the Ariane 5 option; the trajectory followed by the Soyuz option is very similar. In each figure, the plots (a) are in an Earth-centered synodic reference frame (Earth and Lagrange points L_1 and L_2 are represented with dots), while the plots (b) are in an inertial, Sun-centered reference frame (the Sun represented with a dot, and the orbit of the Earth with a solid black line). Note that in plots (b) the z-direction is not to scale with x and y, in order to appreciate the out-of-plane displacement of the pole-sitter, which would otherwise be too small with respect to the orbit of the Earth.

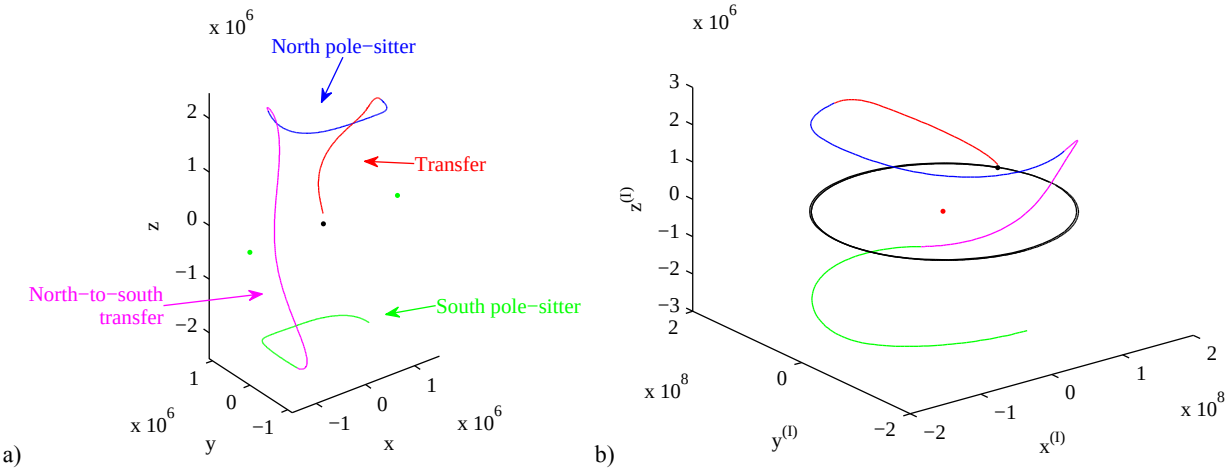

a) b)

Figure 7. Pure SEP mission trajectory (Ariane 5 launch) in synodic reference frame (a) and inertial Sun-centered reference frame (b).

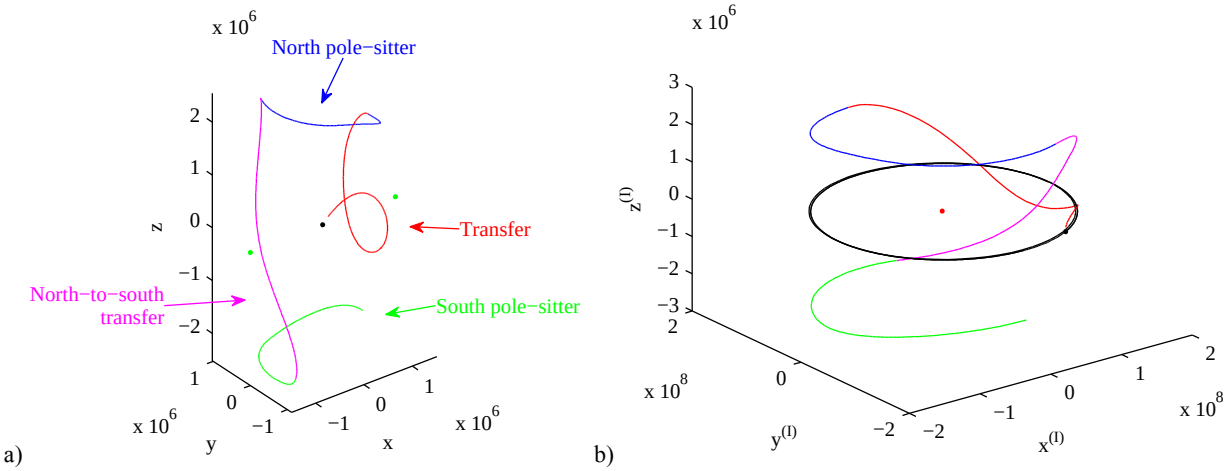

a) b)

Figure 8. Hybrid propulsion mission trajectory (Ariane 5 launch) in synodic reference frame (a) and inertial Sun-centered reference frame (b).

Downloaded From: http://spiedigitallibrary.org/ on 02/14/2013 Terms of Use: http://spiedl.org/terms

4. SPACECRAFT SUBSYSTEMS SIZING

Starting from the total mass m_0 that can be injected into the operational orbit of the pole-sitter (Table 2), a systems design provides the mission lifetime that can be achieved into this orbit, or alternatively the payload mass that can be carried for a given lifetime of the spacecraft. For a preliminary mass budget, the total mass of the pure SEP spacecraft can be split into propellant, tank, SEP thruster, solar arrays, other subsystems and payload. For the hybrid spacecraft, instead, we also consider the gimbal of the SEP thruster, the sail, and the radiators to dissipate any excess of power collected by the sail-mounted thin film solar cells.

Note that the systems mass budget proposed here differs to the one in Ref. [20] in several ways: it considers multiple SEP thrusters, but working in parallel to achieve the necessary thrust, rather than being redundant; the mass of the other subsystems (ADCS, thermal, structure, OBDH, TT&C) is taken into account explicitly, as 30% [1] of the spacecraft dry mass; the pure SEP spacecraft does not employ thin film solar cells, but solar arrays mounted on panels (higher efficiency and areal mass); the pure SEP spacecraft does not employ a gimbal system, as it is assumed that attitude maneuvers can be used to steer the thrust vector; lastly, margins are also taken into account for each subsystem [1]. In particular, the sail and the thin film solar cells are considered new technologies, and therefore a margin of 20% is used. Conversely, the other subsystems are considered to be well-proven technologies, and its margin is set to 5%. The same margin is added to the propellant mass for contingency maneuvers.

Given the initial mass of the spacecraft in the pole-sitter orbit (as found in Table 2 for a given mission scenario), the optimal 1-year trajectory is used to compute the propellant mass m_{prop} needed for a given lifetime $t_{mission}$. Once the propellant mass is found, the mass budget returns the payload mass m_{pl}. This is plotted, as a function of the lifetime, in Figure 9. Each plot refers to one spacecraft architecture (pure SEP, hybrid).

It can be noted that the mission lifetime does not depend on the injected total mass m_0, but only on the technology that is used to build the spacecraft. The lifetime for the pure SEP system is limited to approximately 4.5 years, while this value extends to about 7 years for the hybrid architecture. This result itself should be sufficient to justify the interest in the hybrid propulsion technology for this type of mission, and in general for all those missions which require a continuous acceleration [20]. Furthermore, for nearly equal injected masses, the hybrid spacecraft can carry the same payload mass for a longer mission lifetime. Finally, for a particular spacecraft architecture, the payload mass scales with the injection mass m_0.

Considering a 100-kg payload mass, launching with Soyuz, the lifetime is 3.6 years if the spacecraft is using pure SEP technology, or 5.6 years if using hybrid propulsion. These lifetimes extend to 4.24 and 6.58 years when launching with Ariane 5 for the two architectures respectively.

The subsystem design also allows the computation of the mass of the other subsystems, some of which are reported in Table 3. The size of the total sail assembly (reflective surface and thin film solar cells) of the hybrid spacecraft is 191 m for the Soyuz launch and 324 m for the Ariane launch, assuming a square assembly.

The hybrid configuration furthermore allows a lower power budget, by reducing the thrust needed per unit mass of the spacecraft from the SEP thruster. For the pure SEP spacecraft, the maximum power required by the SEP thruster is 6 kW (Soyuz) and 17.4 kW (Ariane 5). For the hybrid spacecraft, instead, the power is 5.2 kW (Soyuz) and 15 kW (Ariane 5), despite the fact that the total injected mass of the spacecraft, m_0, is slightly larger than in the SEP case.

Downloaded From: http://spiedigitallibrary.org/ on 02/14/2013 Terms of Use: http://spiedl.org/terms

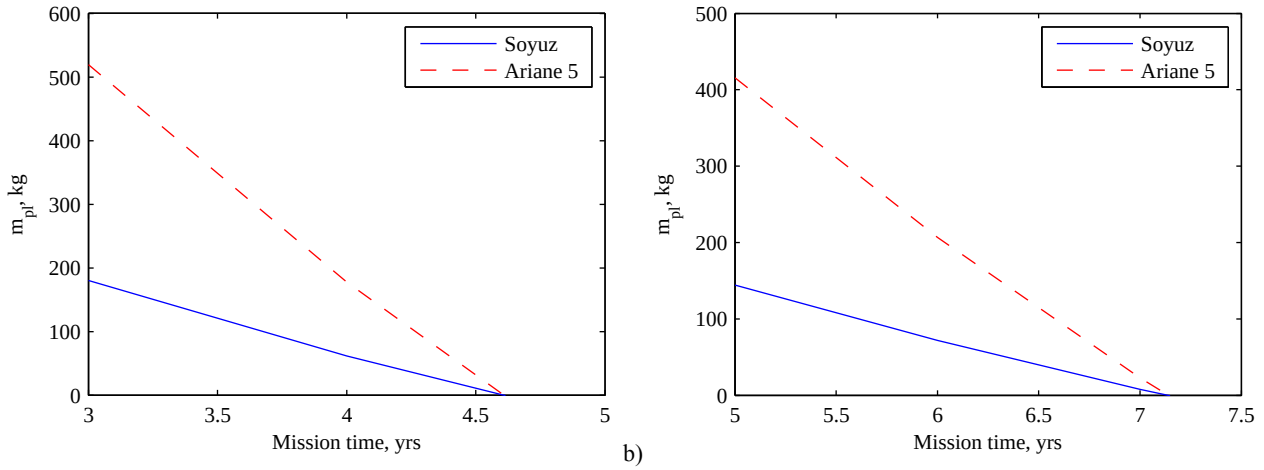

Figure 9. Payload mass (m_{pl}) as a function of the mission lifetime, for the pure SEP spacecraft (a) and the hybrid spacecraft (b).

Table 3. Design points. Masses are without margins.

Architecture	Pure SEP		Hybrid	
Launcher	Soyuz	Ariane 5	Soyuz	Ariane 5
Lifetime, $t_{mission}$, yrs	3.6	4.24	5.6	6.58
Payload mass, m_{pl}, kg	100	100	100	100
Pole-sitter injection mass, m_0, kg	1537	4439	1595	4599
SEP mass, kg	121	348	104	299
Propellant mass, m_{prop}, kg	675	2192	698	2242
Other subsystems mass, kg	259	674	269	707
Solar array/TFSC area, m^2	44	127	121	349
Solar sail mass (reflective), kg	-	-	182	524
Total sail area (reflective + TFSC), m^2	-	-	191 × 191	324 × 324
Maximum SEP thrust, mN	269	776	231	667
Maximum SEP power, kW	6	17.4	5.2	15.0

4.1 Payload Selection and Potential Applications

We now wish to investigate possible payloads that could be used on the pole-sitter spacecraft. As noted in the introduction, the pole-sitter spacecraft could serve as a platform for Earth observation and science, and a data relay for telecommunications. Concerning the former, taking into account the considerable distance of the spacecraft from the Earth, high-resolution imaging is limited to the near-visible part of the spectrum (from infrared to ultra-violet). Figure 10a shows the maximum resolution achievable (limited by diffraction [1], and not taking into account pointing stability of the camera) on the ground from a range of distances, from 30,000 km (about the distance of the geostationary orbit or apogee of typical Molniya orbits) to 3 million km (about the farthest point of the pole-sitter). Clearly, the resolution that can be provided by these two groups of platforms is very different. Spatial resolution in the visible wavelength in the range 10-40 km should be available for the pole-sitter, which enables real-time, continuous views of dynamic phenomena and large-scale polar weather systems [19]. The creation of atmospheric motion vectors (AMV) would also make use of the stationary location of the platform, avoiding gap problems related to geolocation and intercalibration that composite images introduce [5]. Glaciology and ice-pack monitoring would also benefit from continuous, but low resolution polar observation [5]. Ultraviolet imagery of the polar night regions at 100 km resolution or better would enable real-time monitoring of rapidly-changing hot spots in the aurora that can affect high frequency communications and radar [19]. As the resolution degrades with increasing wavelength, it is unlikely that sensing in the microwave band

Downloaded From: http://spiedigitallibrary.org/ on 02/14/2013 Terms of Use: http://spiedl.org/terms

could provide some useful information. However, radio science can detect the total flux of radiation reflected and emitted by the Earth at the poles.

Candidate instruments for continuous polar observations are found in the literature for deep space missions. In fact, optics for deep space mission typically have long focal lengths and narrow filed of views (FOVs), and they are therefore ideal for the pole-sitter. Table 5 collects a number of instruments that were designed for three past missions. In particular, the NASA mission Galileo, launched in 1989 towards Jupiter and its satellites, was designed to perform observations of Jupiter's atmosphere composition, weather phenomena and auroras. Despite that the instruments used on this spacecraft are now outdated, they provide an indication of the data, mass and resolution of the instruments suitable for pole-sitter distances (Figure 11).

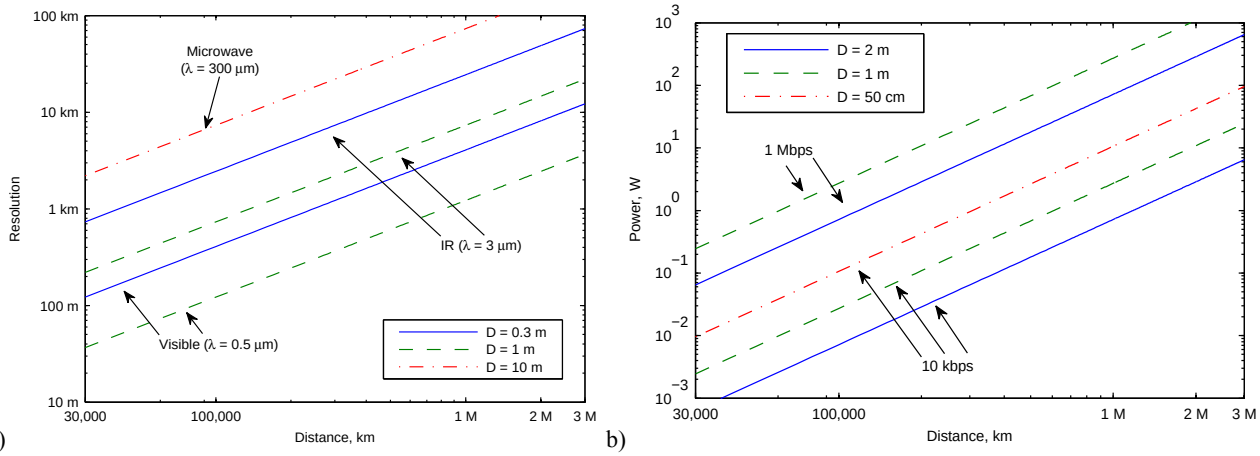

Figure 10. (a) Diffraction-limited resolution as a function of spacecraft distance, for different wavelengths (λ) and instrument aperture diameter (D). (b) Antenna power required as a function of distance, for different spacecraft antenna diameters (D) and data rates.

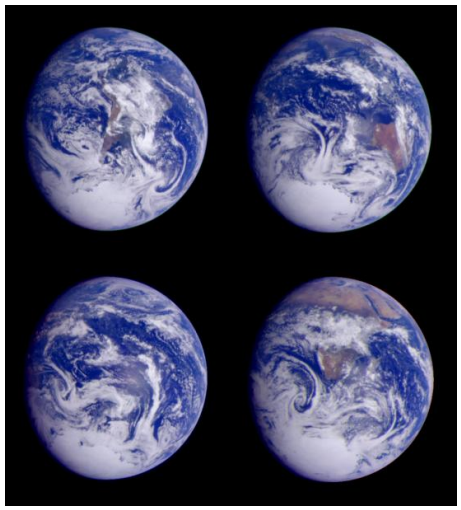

Figure 11. Four views of the Earth as taken by Solid-State Imaging instrument on Galileo spacecraft during its first Earth fly-by, at six-hour intervals on December 11, 1990, at a range of between 2 and 2.7 million kilometers. Each disc is about 500×500 pixels. (Credit: NASA, Johns Hopkins University, http://photojournal.jpl.nasa.gov/catalog/PIA00728)

Downloaded From: http://spiedigitallibrary.org/ on 02/14/2013 Terms of Use: http://spiedl.org/terms

The NASA Deep Space Climate Observatory (DSCOVR) mission was designed for Earth observation and science from the L_1 Lagrange point, which is located approximately 1.5 million km from the Earth, of the same order as the distance of the pole-sitter mission (where angular size of the Earth disc is approximately 0.5 deg). Despite that this mission was initially canceled, its payload would be similar to that which could be used on a pole-sitter spacecraft. Finally, a compact, modern instrument for imaging in the visible and infrared range was successfully flown on the Deep Impact mission. A complete discussion on potential applications enabled by such instrumentation is found in Ref. [2].

Table 5 shows the resolution, wavelength, aperture (to provide an estimate of the size of the instrument), mass and power of each instrument, as well as the main objectives of the instrument within their original mission. The table is interesting as it shows that for all the instruments, the total mass is of the order 50 kg. Therefore, based on Figure 9, they are all suitable for both hybrid and SEP configurations missions, for lifetimes of about 4 years or more.

From the same table it can be noted that the power needed by any of these instruments is two orders of magnitude lower than the power required by the SEP thruster, and therefore should not constitute a strong constraint in the power budget.

Concerning the use of the pole-sitter for telecommunications, the main application would be its use as a low-bandwidth data relay with polar regions, and may be particularly useful in the southern hemisphere, where there are key Antarctic research activities ongoing and communication capabilities are limited. McInnes and Mulligan [5] envisaged possible applications including data links for scientific experiments, links to automated weather stations, emergency airfields and telemedicine. In the same work, the authors proposed the use of polar stationary spacecraft as data relay for future NOAA polar orbiting satellites, such as the NPOESS system. In this case, the telecommunication subsystem would be the main payload of the spacecraft. However, even for Earth science, there will be a need to download a relatively large volume of data from the spacecraft to the Earth real-time (high resolution imaging, for example). Considering the distance of the pole-sitter from the Earth, a high-gain steerable antenna will be required for either or both of these tasks. Table 4, taken from Ref. [1], shows the mass of some parabolic dishes which were used on telecommunication satellites, together with their mass.

Finally, a polar-sitter type platform could be used for high latitude ship tracking and telecommunications, and to support future high-latitude oil and gas exploration, especially if northern sea routes open due to climate change.[*] A complete discussion of possible applications is presented in Ref. [2].

As a final remark, we wish to underline that an accurate determination of the mass of the telecommunication subsystem and the observation payload would require the definition of precise mission objectives, temporal and spatial resolution of the images, and an estimation of the required data-rate. However, for a preliminary definition of spacecraft design points, we consider a mass of 100 kg for both observation and telecommunication payloads (assuming that the RF telecom subsystem is part of the platform mass). With this payload mass, the design points for the four scenarios are described in Table 3. Note that they represent the condition in which the entire capacity of the launcher is used for the pole-sitter spacecraft; however, it is possible to scale down any of the four scenarios (at the cost of a reduction of mission lifetime).

Table 4. Examples of high-gain antennas of telecommunication spacecraft.

Satellite	Type	Band, Frequency	Gain, dBi	Mass, kg	Diameter, m
Intelsat-V	Parabola with Feed Array	C, 4 GHz	21-25	29.4	2.44
Intelsat-V	Parabola with Feed Array	C, 6 GHz	21-25	15.2	1.56
Intelsat-V	Parabola-Steerable	Ku, 11 GHz	36	5.8	1.1
SUPERBIRD	Parabola with Feed Array	Ka, 20/30 GHz	45-52	47.1	1.7

[*] http://www.esa.int/esaEO/SEMT7TRTJRG_index_0.html [cited 17/08/2012].

Downloaded From: http://spiedigitallibrary.org/ on 02/14/2013 Terms of Use: http://spiedl.org/terms

Downloaded From: http://spiedigitallibrary.org/ on 02/14/2013 Terms of Use: http://spiedl.org/terms

Table 5. Potential Earth observation instruments that could be used for polar observation.* Mass and power are also listed, when data are available.

Instrument	Primary objectives	Pixel matrix size/ Field of View/Resolution†	Wavelength	Aperture/ Diameter	Mass, kg	Power
NASA Galileo Primary objective: Study Jupiter and its Moons (1989)						
Solid State Imaging (SSI)	• Cloud structure • Auroral phenomena	800x800 FOV = 0.46 deg (10.16 µrad/pixel) 27 km	Near visible 404-986 nm	30 cm (f/8.5)	29.7 kg	23 W
Near-Infrared Mapping Spectrometer (NIMS)	• Measure reflected sunlight and emitted thermal radiation • Cloud structure	1x20 0.5x10 mrad (0.5 mrad/pixel) 137 km	Infrared 0.7-5.2 µm	22.9 cm (f/3.5)	18 kg	12 W
Ultraviolet Spectrometer (UVS)	• Composition and structure of upper atmosphere	FOV = 0.17 deg	113-432 nm	25 cm	9.7 kg	5.9 W
Photopolarimeter radiometer (PPR)	• Temperature of atmosphere • Distribution of clouds • Distribution of reflected and emitted thermal radiation	FOV = 2.5 mrad	410-892 nm	10 cm	5 kg	11 W
NASA Deep Impact Study the composition of the comet interior of 9P/Tempel (2005)						
High Resolution Instrument (HRI) CCD	• Observe comet nucleus and impact	1008x1008 FOV = 0.118 deg (2 µrad/pixel) 5.4 km	Visible	30 cm (f/35)	N/F‡	N/F§
High Resolution Instrument (HRI) IR spectrometer	• Spectral reflectivity and thermal emission of the nucleus and dust	2.53 mrad x 10 µrad	Infrared 1.05-4.8 µm	f/12	N/F‡	N/F§
NASA Deep Space Climate Observatory (DSCOVR) (formerly Triana) Observation of Sun-lit side of the Earth's disc from L_1 (proposed in 1998)						
Earth Polychromatic Imaging Spectrometer (EPIC)	• Ozone; Aerosols • Cloud fraction, thickness, optical depth, height • Sulfur dioxide • Precipitable water vapor • Volcanic ash • UV irradiance	2048x2048 FOV = 0.62 deg (5.3 µrad/pixel) 14.5 km	Near visible	30.5 cm aperture	39 kg (65 kg with computer)	62 W with computer
Active cavity radiometer (NISTAR)	• Emitted and reflected Earth radiation	FOV = 1 deg	0.2-200 µm	N/A	23.5 kg	N/F

* Data extracted from the official websites of the programs managing agencies.
† Spatial resolution at Nadir from 2.74 million km.
‡ Spacecraft mass: 650 kg
§ Total payload power: 92 W

5. CONCLUSIONS

In this paper a full, preliminary mission analysis and systems design of a near-term and far-term pole-sitter mission is provided, where the distinction comes from the use of either existing, solar electric propulsion (SEP) or more far-term hybrid SEP and solar sail propulsion. The platform would provide a vantage view point on either pole of the Earth, with essentially unlimited temporal resolution (real-time observations) by means of one spacecraft only. Optimal transfers from north to south and vice-versa allow observation of the pole that is lit, at no extra cost in terms of propellant consumption. Moreover, in some particular cases propellant savings can be achieved through the use of these transfers, allowing for an extension of the mission lifetime or alternatively an increase in the payload mass.

The main concern regarding this mission is related to the considerable distance of the spacecraft from Earth. However, it was shown that instruments used on the Galileo mission and others designed for the DSCOVR Earth observation mission from L_1 would enable the observation of large-scale, rapidly-changing weather phenomena, aurorae, ice-pack dynamics, and other phenomena that require only modest spatial resolution. It is also possible also to employ a high-gain antenna to use the spacecraft as a continuous data-relay with scientific stations in the Antarctic and other high-latitude users. Using the full potential of either a Soyuz or Ariane 5 launch vehicle, a systems mass budget demonstrated that it is potentially possible to maintain these payloads in the pole-sitter orbit for at least 4 years for the short-term SEP-only mission, and 6 years or more for the far-term hybrid mission.

ACKNOWLEDGEMENTS

This work was funded by the European Research Council, as part of project 227571 VISIONSPACE. The authors thank Dr. Victor M. Becerra, of the School of Systems Engineering, University of Reading, Reading, UK for providing the software PSOPT freely, as well as advices on its use. Many thanks also to Alex Coletti, of SMRC, for valuable discussions on instruments for polar observation and for providing some of the data presented in this paper.

REFERENCES

[1] Wertz, J. R., and Larson, W. J., [Space mission analysis and design, third edition] Microcosm press/Kluwer Academic Publishers, El Segundo, California, USA (1999).

[2] Ceriotti, M., Diedrich, B. L., and McInnes, C. R., "Novel mission concepts for polar coverage: an overview of recent developments and possible future applications," Acta Astronautica 80, 89-104 (2012).

[3] Anderson, P. C., and Macdonald, M., "Extension of the Molniya orbit using low-thrust propulsion," proc. 21st AAS/AIAA Space Flight Mechanics Meeting, (2011).

[4] Anderson, P. C., and Macdonald, M., "Extension of Earth orbits using low-thrust propulsion," proc. 61st International Astronautical Congress (IAC 2010), (2010).

[5] McInnes, C. R., and Mulligan, P., [Final report: telecommunications and Earth observations applications for polar stationary solar sails] National Oceanographic and Atmospheric Administration (NOAA)/University of Glasgow, Department of Aerospace Engineering, (2003).

[6] Driver, J. M., "Analysis of an arctic polesitter," Journal of Spacecraft and Rockets 17(3), 263-269 (1980).

[7] McInnes, C. R., [Solar sailing: technology, dynamics and mission applications] Springer-Verlag, Berlin (1999).

[8] Mori, O., Sawada, H., Funase, R., Endo, T., Morimoto, M., Yamamoto, T., Tsuda, Y., Kawakatsu, Y., and Kawaguchi, J. i., "Development of first solar power sail demonstrator - IKAROS," proc. 21st International Symposium on Space Flight Dynamics (ISSFD 2009), (2009).

[9] Johnson, L., Whorton, M., Heaton, A., Pinson, R., Laue, G., and Adams, C., "NanoSail-D: A solar sail demonstration mission," Acta Astronautica 68(5-6), 571–575 (2011).

[10] Ceriotti, M., and McInnes, C. R., "Generation of optimal trajectories for Earth hybrid pole-sitters," Journal of Guidance, Control, and Dynamics 34(3), 847-859 (2011).

[11] Forward, R. L., "Statite: a spacecraft that does not orbit," Journal of Spacecraft and Rockets 28(5), 606-611 (1991).

[12] Waters, T. J., and McInnes, C. R., "Periodic orbits above the ecliptic in the solar-sail restricted three-body problem," Journal of Guidance, Control, and Dynamics 30(3), 687-693 (2007).

[13] Leipold, M., and Götz, M., [Hybrid photonic/electric propulsion] Kayser-Threde GmbH, Munich, Germany (2002).

[14] Baig, S., and McInnes, C. R., "Artificial three-body equilibria for hybrid low-thrust propulsion," Journal of Guidance, Control, and Dynamics 31(6), 1644-1655 (2008).

[15] Mengali, G., and Quarta, A. A., "Trajectory design with hybrid low-thrust propulsion system," Journal of Guidance, Control, and Dynamics 30(2), 419-426 (2007).

Downloaded From: http://spiedigitallibrary.org/ on 02/14/2013 Terms of Use: http://spiedl.org/terms

[16] Mengali, G., and Quarta, A. A., “Tradeoff performance of hybrid low-thrust propulsion system,” Journal of Spacecraft and Rockets 44(6), 1263-1270 (2007).
[17] Simo, J., and McInnes, C. R., "Displaced periodic orbits with low-thrust propulsion," proc. 19th AAS/AIAA Space Flight Mechanics Meeting, (2009).
[18] Heiligers, J., Ceriotti, M., McInnes, C. R., and Biggs, J. D., “Displaced geostationary orbit design using hybrid sail propulsion,” Journal of Guidance, Control, and Dynamics 34(6), 1852-1866 (2011).
[19] Lazzara, M. A., Coletti, A., and Diedrich, B. L., “The possibilities of polar meteorology, environmental remote sensing, communications and space weather applications from Artificial Lagrange Orbit,” Advances in Space Research 48(11), 1880-1889 (2011).
[20] Ceriotti, M., and McInnes, C. R., “Systems design of a hybrid sail pole-sitter,” Advances in Space Research 48(11), 1754–1762 (2011).
[21] Heiligers, J., Ceriotti, M., McInnes, C. R., and Biggs, J. D., “Design of optimal Earth pole-sitter transfers using low-thrust propulsion,” Acta Astronautica 79, 253–268 (2012).
[22] Heiligers, J., Ceriotti, M., McInnes, C. R., and Biggs, J. D., "Design of optimal transfers between North and South pole-sitter orbits," proc. 22nd AAS/AIAA Space Flight Mechanics Meeting, (2012).
[23] Kaplan, M. H., [Modern spacecraft dynamics and control] John Wiley and Sons, Inc., New York (1976).
[24] Brophy, J., “Advanced ion propulsion systems for affordable deep-space missions,” Acta Astronautica 52(2-6), 309-316 (2003).
[25] Leiter, H. J., Killinger, R., Bassner, H., Müller, J., Kukies, R., and Fröhlich, T., "Development and performance of the advanced radio frequency ion thruster RIT-XT," proc. 28th International Electric Propulsion Conference (IEPC 2003), (2003).
[26] Marcuccio, S., Paita, L., Saviozzi, M., and Andrenucci, M., [Flight demonstration of FEEP on get away special] AIAA, Cleveland, OH, USA (1998).
[27] Funase, R., Mori, O., Tsuda, Y., Shirasawa, Y., Saiki, T., Mimasu, Y., and Kawaguchi, J., "Attitude control of IKAROS solar sail spacecraft and its flight results," proc. 61st International Astronautical Congress (IAC 2010), (2010).
[28] Dachwald, B., Mengali, G., Quarta, A. A., and Macdonald, M., “Parametric model and optimal control of solar sails with optical degradation,” Journal of Guidance, Control, and Dynamics 29(5), 1170-1178 (2006).
[29] Kawaguchi, J. i., Mimasu, Y., Mori, O., Funase, R., Yamamoto, T., and Tsuda, Y., "IKAROS - Ready for lift-off as the world's first solar sail demonstration in interplanetary space," proc. 60th International Astronautical Congress (IAC 2009), (2009).
[30] Murphy, D. M., Murphey, T. W., and Gierow, P. A., “Scalable solar-sail subsystem design concept,” Journal of Spacecraft and Rockets 40(4), 539-547 (2003).
[31] Becerra, V. M., [PSOPT optimal control solver user manual], (2009).

Downloaded From: http://spiedigitallibrary.org/ on 02/14/2013 Terms of Use: http://spiedl.org/terms